Journal of Materials Chemistry A

High Temperature Superconducting Materials as Bi-functional Catalysts for Hydrogen Evolution and Oxygen Reduction

Journal:	*Journal of Materials Chemistry A*
Manuscript ID:	TA-ART-12-2014-006767.R1
Article Type:	Paper
Date Submitted by the Author:	08-Feb-2015

Complete List of Authors:	Lim, Chee Shan; Nanyang Technological University, Chemistry and Biological Chemistry Chua, Chun Kiang; Nanyang Technological University, Chemistry and Biological Chemistry Wang, Lu; Nanyang Technological University, Chemistry and Biological Chemistry Sofer, Zdenek; Institute of Chemical Technology, Jankovský, Ondřej; Institute of Chemical Technology, Dept. of Inorganic Chemistry Pumera, Martin; Nanyang Technological University, Chemistry and Biological Chemistry

Journal Name

RSCPublishing

ARTICLE

High Temperature Superconducting Materials as Bi-functional Catalysts for Hydrogen Evolution and Oxygen Reduction

Cite this: DOI: 10.1039/x0xx00000x

Received 00th January 2012,
Accepted 00th January 2012

DOI: 10.1039/x0xx00000x

www.rsc.org/

Chee Shan Lim[a], Lu Wang[a], Chun Kiang Chua[a], Zdeněk Sofer[b], Ondřej Jankovský[b], Martin Pumera*[a]

As the world progresses towards green and cost-effective energy applications, it is imperative to discover and introduce viable electrocatalysts to replace platinum, which is expensive and scarce. The group of high-temperature superconductors has been intensively studied at the end of 20th century owing to their unique electrical behaviour; nonetheless, we wish to show their interesting electrocatalytic properties as well. This work seeks to investigate the feasibility of two high-temperature superconductors, $YBa_2Cu_3O_7$ (YBCO) and $Bi_2Sr_2CaCu_2O_8$ (BSCCO) in catalysing hydrogen evolution and oxygen reduction reactions electrochemically. These materials can be easily synthesized by solid state reaction and in combination with fairly impressive electrocatalytic properties displayed in our study, they definitely possess the potential to replace platinum as prospective electrocatalysts.

1. Introduction

Renewable and environmentally-benign sources of energy have been intensively researched on for industrial technologies such as fuel cells, energy-storage as well as water-splitting following the woes of dwindling resources which have been plaguing the world over the past decades. Amongst the array of alternatives, electrochemical processes including hydrogen evolution reaction (HER) and oxygen reduction reaction (ORR) are fervently investigated to generate energy carriers for these important applications.[1–4] Hydrogen is a clean, and sustainable fuel source with, by far, the largest current density and it is currently widely used as a replacement for fossil fuels as energy carriers for fuel cell applications. Hydrogen evolution can be performed electrochemically in an acidic medium which follows the general equation: $2H^+ + 2e^- \rightarrow H_2$. This process basically involves two steps, the adsorption and desorption step. The former occurs when protons are adsorbed onto the electrode surface, whereas the latter involves the desorption of molecular hydrogen from the electrode surface.[5] The bonding strength between the hydrogen and electrode surface determines the limiting step in this process, but in general, the overall rate of reaction is largely dependent on the free energy of hydrogen adsorption, ΔG_H.[6] On the other hand, reduction of earth-abundant oxygen to water plays a vital role in next-generation zinc batteries and many other energy-converting systems.[7] Reduction of oxygen can be carried out in both acidic and alkaline media; in the alkaline medium, molecular oxygen can be reduced *via* either a 4-electron ($O_2 + 2H_2O + 4\ e^- \rightarrow 4OH^-$) or two 2-electron ($O_2 + H_2O + 2e^- \rightarrow HO_2^- + OH^-$; $HO_2^- + H_2O + 2\ e^- \rightarrow 3OH^-$) processes.[8]

Despite the great benefits brought forth by these electrochemical processes, the slow kinetics of these processes impedes the rate of reaction and affects bulk commercialisation of related energy applications.[9] Efficient electrocatalysts are therefore required to enhance the reaction rates and improve the overall reaction outcome. Platinum has been the best-performing electrocatalyst for these reactions till date,[10,11] but its rarity and cost have put off the electrochemical community. These drawbacks have sparked an ongoing search for alternative catalysts that are highly available and can possibly rival the electrocatalytic performance of platinum. A wide range of catalysts with promising electrocatalytic properties close to that of platinum for HER and ORR have since been discovered, including metal-based nanoparticles, layered materials and graphene-based materials.[12–19]

Similar to layered cobaltites,[20,21] cuprates seem to be promising candidates for HER and ORR as well. Therefore, emphasis has been placed on two different cuprates, $YBa_2Cu_3O_7$ (YBCO) and $Bi_2Sr_2CaCu_2O_8$ (BSCCO) in this work. These cuprates belong to a group of high-temperature superconductors (HTSCs). YBCO, with a general chemical formula of $YBa_2Cu_3O_{7-\delta}$, is a HTSC discovered in 1987 with T_C~90 K.[22] As shown in Figure 1A, the structure of YBCO is related to the family of

perovskites with space group *Pmmm*.[23] On the other hand, BSCCO, the first HTSC that does not contain any rare earth elements is a HTSC discovered by Maeda et. al. in 1988.[24] Its structure is defined by a layered system belonging to the homologous series $Bi_2Sr_2Ca_{n-1}Cu_nO_{2n+4}$ with the *Amaa* symmetry as displayed in Figure 1B.

In this work, we synthesized YBCO and BSCCO by solid state reaction and characterised the structure using X-ray diffraction and scanning electron microscopy. The bulk and surface composition were also deduced by energy dispersive X-ray spectroscopy and X-ray photoelectron spectroscopy. Subsequently, we investigated the potentials of the two materials as viable catalysts for hydrogen evolution and oxygen reduction reactions using linear sweep voltammetry (LSV) and cyclic voltammetry (CV) respectively.

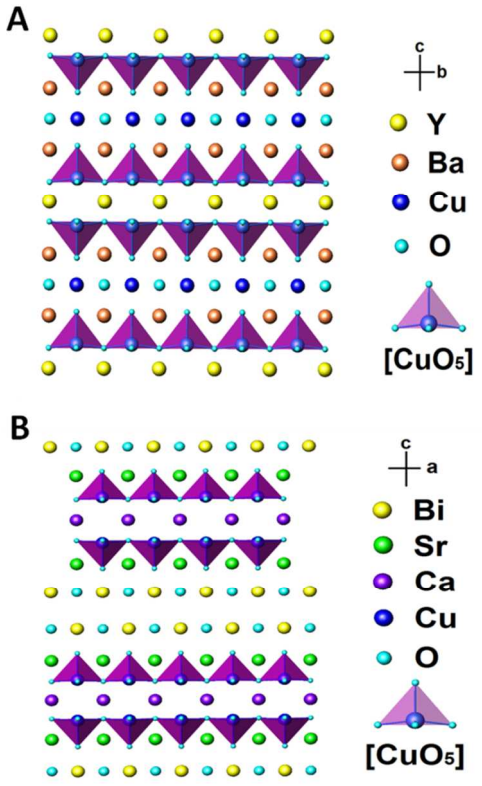

Figure 1 Structure of (A) YBCO and (B) BSCCO.

2. Experimental

2.1 Materials

Y_2O_3, $BaCO_3$, CuO, Bi_2O_3, $SrCO_3$ and $CaCO_3$ used for the synthesis of YBCO and BSCCO were obtained from Sigma-Aldrich, Czech Republic. Oxygen of 99.9% purity was obtained from SIAD, Czech Republic.

N,N-dimethylformamide (DMF), sodium chloride, potassium chloride, sodium phosphate dibasic, potassium phosphate monobasic, platinum on graphitized carbon, nafion 117 solution, sulfuric acid (55-98 %, v/v) and potassium hydroxide were purchased from Sigma-Aldrich, Singapore. The modulated speed rotator set-up (model PGSTAT302M) and the rotating-ring disk electrode (RRDE) with a diameter of 5.6 mm were obtained from Pine, Durham, USA. Glassy carbon (GC) electrodes with a diameter of 3 mm were obtained from Autolab, The Netherlands. The Milli-Q water with a resistivity of 18.2 MΩcm was used throughout the experiments.

2.2 Instrumentation

X-Ray diffraction (XRD) patterns were collected at room temperature on X'Pert PRO θ-θ powder diffractometer with parafocusing Bragg-Brentano geometry using CuKα radiation (λ=1.5418 Å, U=40 kV, I=30mA).

Scanning electron microscopy (SEM) was carried out with Jeol 7600F SEM (Jeol, Japan) operating at 2 kV in GB high to investigate the morphology of the materials.

Energy-dispersive X-ray spectroscopy (EDS) was recorded on a Jeol 7600F (Jeol, Japan) at 15 kV to obtain the elemental composition and mapping of the material.

X-ray photoelectron spectroscopy (XPS) measurements were acquired using a Phoibos 100 spectrometer and a monochromatic Mg X-ray radiation source (SPECS, Germany). Survey scans and high-resolution spectra of the various metals and C1s were measured to determine the atomic percentage of each metal in the doped GO. Samples were prepared by affixing the material onto an aluminium XPS sample holder using a sticky conductive carbon tape. The layer of material was ensured to be uniform throughout.

Linear sweep voltammetry (LSV) and *cyclic voltammetry (CV)* measurements were carried out with a μAutolab type III electrochemical analyser (Eco Chemie, The Netherlands) connected to a personal computer and controlled by NOVA 1.8 software. All voltammetry experiments were performed in a 5 mL electrochemical cell at room temperature using a three-electrode configuration. A platinum electrode functioned as an auxiliary electrode while an Ag/AgCl electrode was utilised as a reference electrode. All electrochemical potentials in this paper are stated *vs.* the Ag/AgCl reference electrode unless otherwise stated in the figures.

2.3 Procedure

YBCO was synthesized from Y_2O_3, $BaCO_3$ and CuO by the solid state reaction. Powders were weighed and mixed in an agate mortar in ratios corresponding to the overall composition $YBa_2Cu_3O_7$. They were calcined for 48 hr at 940 °C in air with the heating and cooling rate of 5 °C min^{-1}. Calcined powder was ground in agate mortar and heated in oxygen for 48 hours at 940 °C with the heating and cooling rate of 5 °C min^{-1}. After the final calcination and homogenization, the powder was pressed into pellets under the pressure of 300 MPa. The pellets were sintered under oxygen atmosphere at 900 °C for 48 hr and slowly cooled (cooling rate of 0.1 °C min^{-1}) to room temperature.

BSCCO with the composition $Bi_2Sr_2CaCu_2O_8$ was also synthesized by the solid state reaction from pure CuO, Bi_2O_3, $SrCO_3$ and $CaCO_3$. The powders were mixed, homogenized and calcined thrice at 700 °C, 750 °C and 800 °C, respectively with

the heating and cooling rate of 5 °C min^{-1}. After each calcination step, the powder was again manually homogenized. Following the final calcination and homogenization, the powder was pressed into pellets under the pressure of 300 MPa. The pellets were sintered in air atmosphere at 850 °C with the heating and cooling rate of 5 °C min^{-1}.

Cyclic voltammetry measurements were taken at a scan rate of 0.1 V s^{-1} for inherent electrochemistry scans. Linear sweep voltammetry measurements were recorded at a scan rate of 0.002 V s^{-1} and 0.005 V s^{-1} for hydrogen evolution reaction in 0.5 M sulfuric acid, and oxygen reduction reaction in 0.1 M potassium hydroxide using the GC electrodes respectively. Linear sweep voltammetry measurements were also recorded on the RRDE for ORR reaction under the same conditions as GC, with rotation speeds ranging from 500 rpm and 2000 rpm at intervals of 250 rpm. The reproducibility of the measurements was obtained over 3 experiments each time, using 3 different electrode units.

All electrode surfaces were renewed by polishing with 0.05 µm alumina powder on a polishing pad. A suspension of the desired material with a concentration of 1 mg mL^{-1} in DMF and 1 mg mL^{-1} in 0.1 wt% nafion for measurements carried out in GC and RRDE respectively was first prepared, followed by a 60 min ultrasonication. A micropipette was then used to deposit 1 µL and 10 µL aliquot of the appropriate suspension onto the GC and RRDE electrode surfaces respectively to immobilise the material onto the working electrode. Upon evaporation of the solvent at room temperature, a randomly distributed film was obtained on the glassy carbon electrode surface, with a catalyst loading of 0.014 mg cm^{-2}. The catalyst loading onto the RRDE for the determination of electrons transferred during ORR was 0.040 mg cm^{-2}.

3. Results and Discussion

Prior to analysis on their electrocatalytic properties, the materials were first characterised. Successful synthesis of the materials was proven firstly by the X-ray diffraction technique. The XRD diffractograms of both YBCO and BSCCO are shown in Figure 2. Red vertical lines in both diffractograms were plotted in the figures to compare the purity of prepared samples to previously published XRD references.[25,26] In the first sample (Figure 2A), only the $YBa_2Cu_3O_7$ phase was detected. Whereas in the second sample (Figure 2B), two small peaks belonging to another phase at 2θ=21.75 and 25.83 were detected other than the $Bi_2Sr_2CaCu_2O_8$ phase. These peaks probably belong to the phase $Bi_2Sr_2CuO_6$; however, the content of this phase is very low (~2 wt%), deeming the amount of sample present in the $Bi_2Sr_2CuO_6$ form negligible.

The morphology of the materials was established using the SEM technique, as exhibited in Figure 3. Cuboid-shaped grains of YBCO (Figures 3A, B) were detected reflecting the high symmetric space group *Pmmm*. On the other hand, layers of BSCCO were apparent from Figures 3C and D, with well-established thickness of < 2 µm.

Elemental analysis was subsequently carried out with EDS to further characterise the composition of materials. The EDS spectra obtained are displayed in Figure 4. Elements in YBCO are apparent in the EDS spectra (Figure 4A), and these elements, yttrium, barium, copper and oxygen have constituted 7.6 at%, 16.2 at%, 23.2 at% and 53.0 at% of the sample. These proportions correspond to the overall composition of $YBa_{2.13}Cu_{3.05}O_{6.97}$, confirming successful synthesis of required phase (yttrium stoichiometry was fixed to 1).

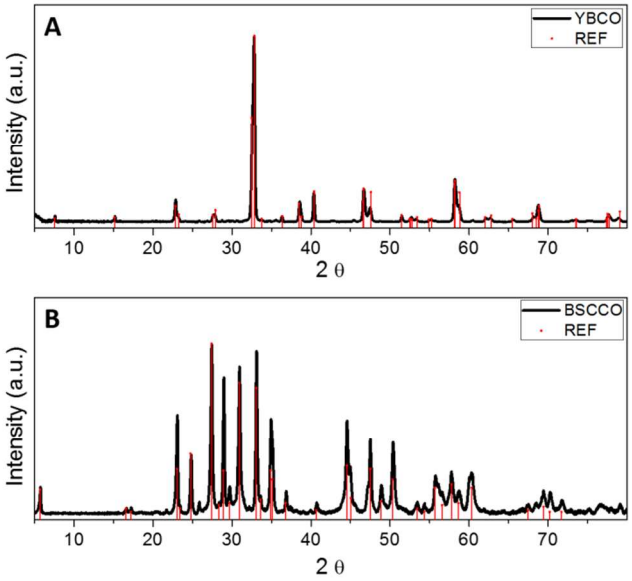

Figure 2 XRD patterns of (A) YBCO and (B) BSCCO compared to previously published diffractograms.

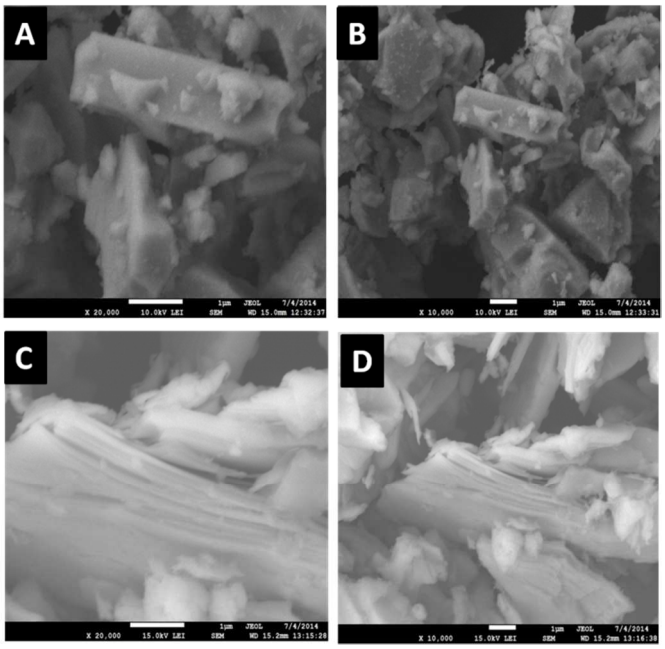

Figure 3 SEM images of (A,B) YBCO and (C,D) BSCCO at magnifications of 20,000 x and 10,000 x, respectively.

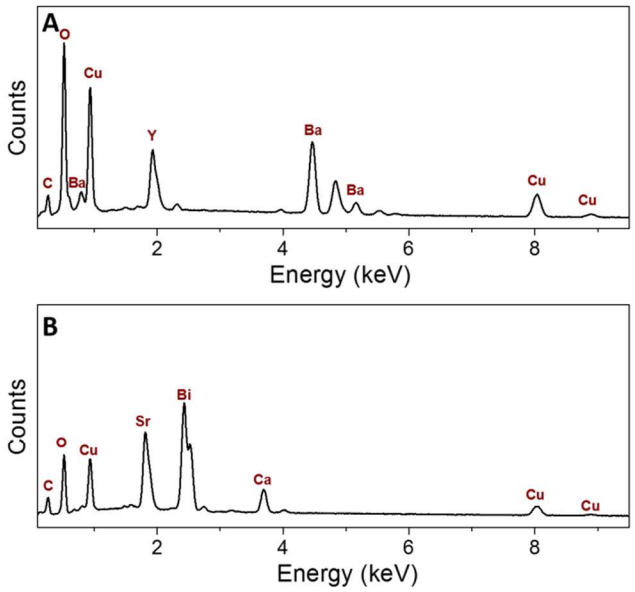

Figure 4 SEM/EDS spectra of (A) YBCO and (B) BSCCO.

Figure 4B displays the EDS spectra of BSCCO. The presence of 13.1 at% of bismuth, 10.3 at% of strontium, 7.7 at% of calcium, 13.6 at% of copper and 55.3 at% of oxygen was found in the sample, with no impurities detected. By fixing the stoichiometry of Bi=2, we concluded the composition of the sample to be $Bi_2Sr_{1.57}Ca_{1.18}Cu_{2.08}O_{8.44}$. Evidences of carbon were also observed in both samples; these could originate from the double-sided carbon tape used for sample holding.

Finally, XPS was done to extract information on the surface composition of YBCO and BSCCO. The chemical environments/oxidation states of the elements were determined from the high resolution scans in Figure 5.

YBCO Figure 5A shows the high resolution spectra of elements in YBCO. Two sets of peaks are present in the most intensive core-level emission state of yttrium, Y3d. The shallower set occurs at 158.0 eV and 160.1 eV for $3d_{5/2}$ and $3d_{3/2}$ and the other at 160.4 eV and 162.5 eV, respectively. The former can be attributed to the Y_2O_3 surface, despite differing from literature by about 1 eV.[27] Both components have almost identical spin-orbit splitting (δ) of 2.1 eV, which matches results reported previously (2.05 eV). For Ba3d high resolution spectrum, the $3d_{5/2}$ peak at 779.2 eV coincides with that of Ba-O surface.[28] An apparent second $3d_{5/2}$ peak is located at 781.8 eV. This is likely due to the presence of Ba^{2+} in the material. The Cu2p spectrum consists of a set of main peaks and a broader satellite set. The main $2p_{3/2}$ peak at 934.6 eV denotes the Cu-O surface, whose binding energy value is believed to be at 933.5 eV from past studies.[29] The intensity ratio of the satellite and main peak (I_{sat}/I_{main}) is measured to be about 0.41. This is within the characteristic YBCO range of 0.38–0.45. The peak position and intensity ratio appear to indicate the existence of Cu^{2+} and Cu^{3+} in copper as well.[30] The O1s spectrum shows 3 peaks, at 528.6 eV, 530.6 eV and 533.0 eV. The first peak with the lowest binding energy falls within the range of 528–528.5 eV, a region characteristic of oxygen in Cu-O and CuO_2 surfaces in YBCO.[31] Presence of this peak is the best indication of the successful synthesis of YBCO, as it also corresponds to the BaO signal. The remaining peaks show oxygen in various environments that cannot be pinpointed specifically. Possible deductions include Y_2O_3 and hydroxides.

BSCCO High resolution spectra of the respective elements in BSCCO are presented in Figure 5B. The core-level spectrum of Bi4f is split into 2 portions (Bi $4f_{7/2}$ and Bi $4f_{5/2}$) in a ratio of 4:3 due to spin-orbit coupling. The first set of $4f_{7/2}$ and $4f_{5/2}$ peaks occur at 158.3 eV and 163.8 eV, respectively, with a peak separation of about 5.5 eV. This result matches closely to that from previous studies.[32] The second set of peaks at 160.9 eV ($4f_{7/2}$), though not the emphasis in BSCCO studies might be attributed to the Bi_2O_3 environment. The Sr3d core-level spectrum shows two sets of $3d_{5/2}$ and $3d_{3/2}$ peaks. The binding energy of the first $3d_{5/2}$ peak is at 132.4 eV with the corresponding $3d_{3/2}$ peak at 133.7 eV. The shift of energy is calculated to be about 1.3 eV, concurring with that proposed by Meyer III and co.[33] The second set of peaks at 135.0 eV for $3d_{5/2}$ suggests the presence of Sr-O bonding.[34] As for the Ca2p high resolution spectrum, 2 components of spin-orbit coupling at 347.0 and 350.5 eV, as well as 348.9 and 352.4 eV for $2p_{3/2}$ and $2p_{1/2}$ respectively. The latter is believed to be due to inequivalent Sr/Ca lattice sites as proposed previously.[35] Both sets of peaks have almost identical spin-orbit splitting, δ, of 3.5 eV, suggesting the presence of calcium in two different environments. This environment is likely to arise from Ca-O interaction.[36] The Cu2p spectrum exhibits two sets of peaks, one for the main signal and the other, the satellites. The main $2p_{3/2}$ peak occurs well in agreement with literature at 933.6 eV, with an approximate energy shift of 9.7 eV between itself and the corresponding satellite peak.[37] The main peaks denote a well-screened core-hole at $2p^53d^{10}L$ and the occurrence of the satellite peaks is possibly due to a poorly screen $2d^53d^9$ configuration, where L represents the hole on oxygen lattice sites. Finally, 3 peaks were observed at the O1s spectrum, with binding energies of 528.1 eV, 530.5 eV and 532.9 eV. The main peak at 528.1 eV is known as a characteristic peak for well-performing HTSC surfaces,[38] as it also depicts the Cu-O environment.[33] Remaining peaks suggest other possible oxygen bonding such as Sr-O and Bi-O.

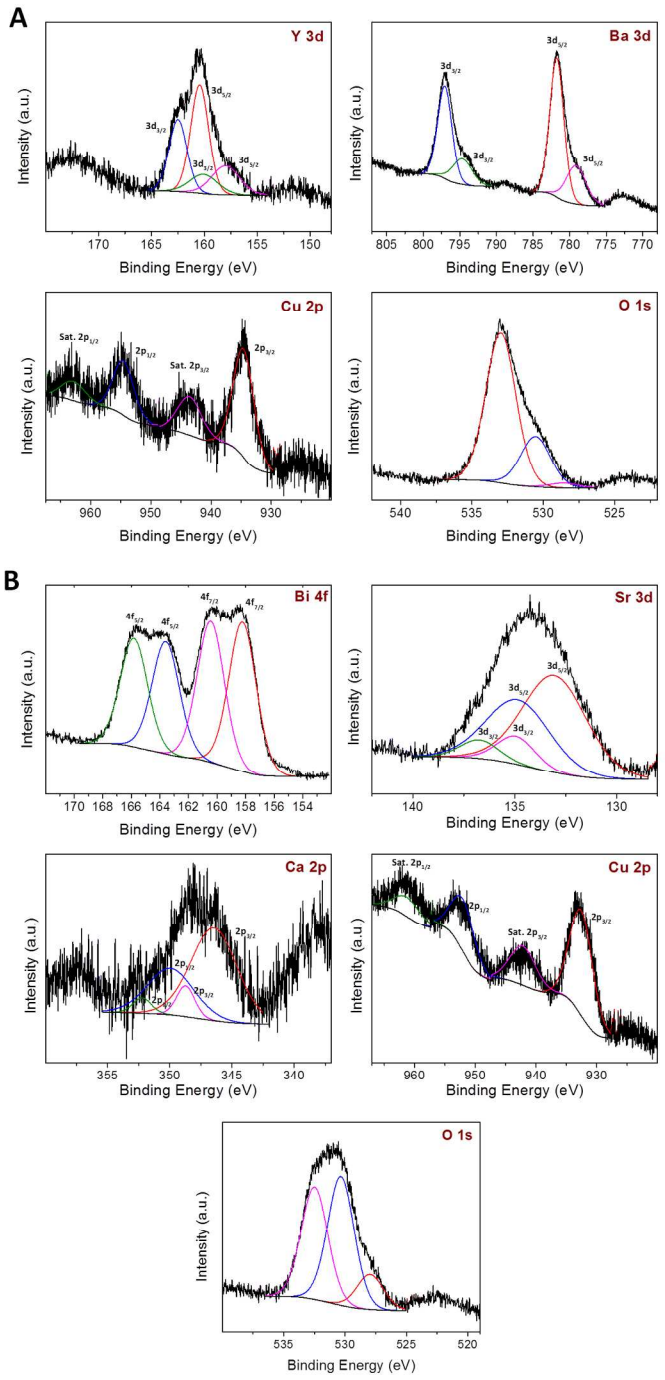

Figure 5 XPS high resolution spectra of (A) YBCO and (B) BSCCO.

With the structure and composition of the materials ascertained, the inherent electrochemistry of the materials was studied next. From Figures 6A and B, three intrinsic reduction peaks are evident in both materials between +0.7 V to –1.3 V, deeming both YBCO and BSCCO electroactive in nature. Increments of the peak heights are also observed with each consecutive scan, indicating that oxidation is also taking place in the reverse direction despite negligible oxidation signals present. The

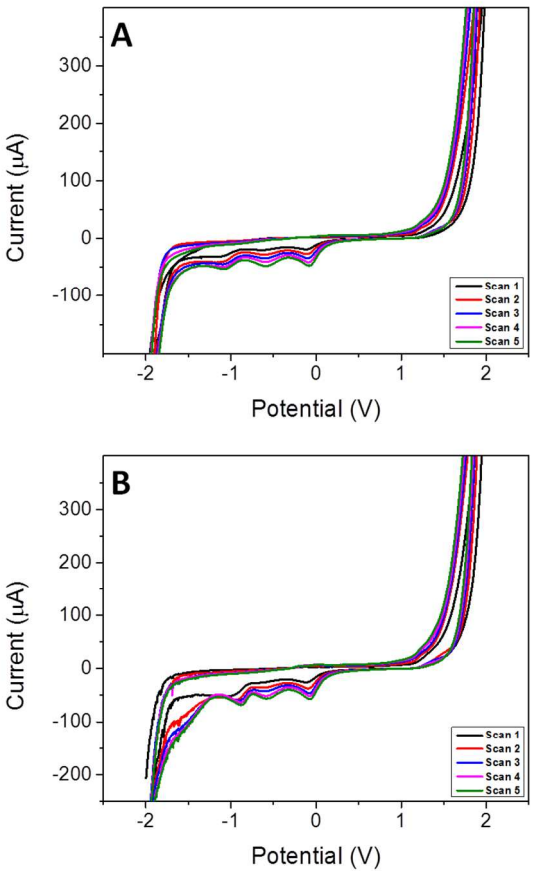

Figure 6 Cyclic voltammograms of PBS background electrolyte (50 mM, pH 7.2) on (A) YBCO and (B) BSCCO surfaces for five consecutive scans in the anodic direction. Conditions: Scan rate 100 mV s^{-1}. No analyte was added.

reduction peaks correspond to that of Cu^{3+}, which has been proven to generate three reduction peaks in layered materials.

The electrocatalytic potentials of the two materials were subsequently studied. Oxygen reduction reaction was firstly carried out, and the results were put in comparison against Pt/C and bare glassy carbon surfaces. Sensitivity of the surfaces was examined using the peak current attained in Figure 7A. The Pt/C-modified surface obtained the largest peak current value of 3.93 μA, while the peak current values for the YBCO– and BSCCO–modified surfaces were smaller at about 2.99 μA and 3.51 μA, respectively. Despite so, the peak current values of the layered materials proved to be much higher than that of bare GC surface (2.62 μA), indicating relatively fine electrochemical performance as the peak current is an indicator of the electron transfer during the reaction. Onset potential of the oxygen reduction reaction was also determined and summarised in Figure 7B to compare the reaction rates among the surfaces. Pt/C continues to display extraordinary electrocatalytic performance with the earliest onset potential (–211 (±4) mV) achieved, followed by YBCO and BSCCO at –272 (±9) mV and –278 (±8) mV, respectively. YBCO appears to be a slightly better electrocatalyst between the two layered materials in this case, though both of them performed much better than bare GC surface (–282 (±10) mV). The Pt/C results concur with that of

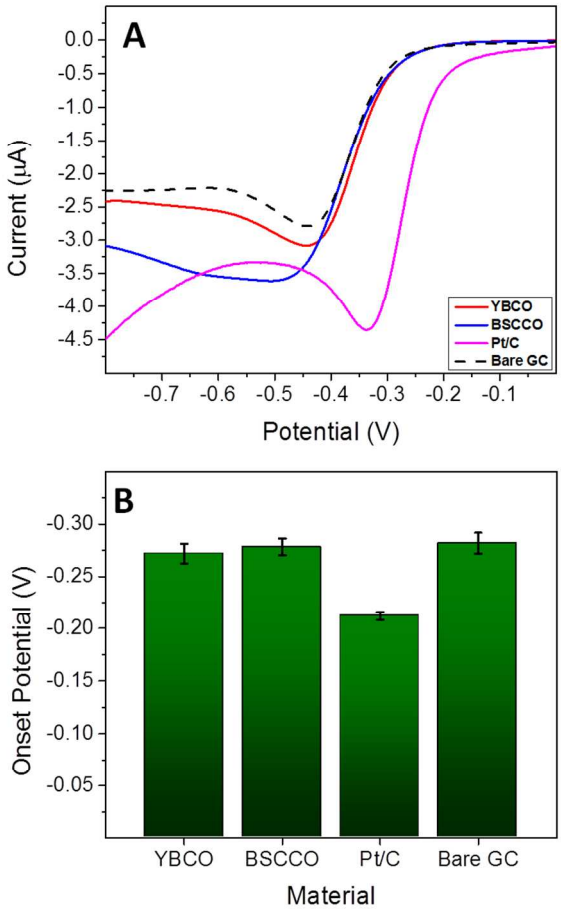

Figure 7 (A) Linear sweep voltammograms of oxygen reduction on YBCO, BSCCO, Pt/C and bare GC and (B) their respective onset potential values. Conditions: 0.1 M potassium hydroxide, scan rate 5 mV s^{-1}.

previous works to a large extent,[39] hence affirming the accuracy of the results obtained in this work. Koutecky-Levich analysis was subsequently performed using the rotating-ring disk electrode. The amount of electrons transferred yielded was 2.19 for YBCO and 2.82 for BSCCO. It is important to note that the Koutecky-Levich equation is derived for flat electrodes and its application for nanomaterials–modified electrodes can lead to skewed or unreliable results, as demonstrated by Compton and co-workers lately.[40]

The electrocatalytic capabilities of the layered materials were further affirmed using hydrogen evolution reaction in acidic medium. Figure 8 illustrates the electrocatalytic performances of the materials using current density as the parameter. Onset of the hydrogen evolution occurred at around the same potential for both layered materials, at about –0.65 V (*vs* RHE). This onset potential is much later than that of Pt/C, but evidently earlier than bare GC, indicating that the layered materials possess promising electrocatalytic capabilities in hydrogen evolution. Between the two layered superconductors, YBCO appears to be a more competent alternative for ORR and HER than BSCCO. Nonetheless, it is undeniable that BSCCO is definitely a viable replacement for Pt/C as well, judging from

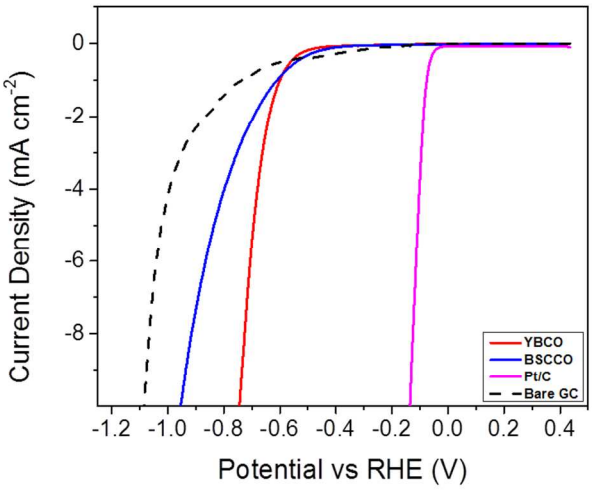

Figure 8 Linear sweep voltammograms of hydrogen evolution Conditions: 0.5 M sulfuric acid, scan rate 2 mV s^{-1}.

its dominance against the bare GC surface in both reactions. There have also been numerous schemes which make use of hydrogen reduction as an indication for biorecognition events; YBCO and BSCCO materials can be used in such schemes as well.[41]

The chemical stability of cuprates towards moistness and influence of carbon dioxide has been investigated previously.[42] Long term exposure of YBCO to water and carbon dioxide has led to the formation of barium hydroxide and barium carbonate on the surfaces. It was also described that a co-substitution of Ca^{2+} for Y^{3+} and La^{3+} for Ba^{2+} in YBCO can improve its resistivity against corrosion.[43] The corrosion effect takes place only on the surface, with negligible effects on the bulk chemical stability. The extent of material degradation in acidic or alkaline environment will be a subject for further studies. Nonetheless, we believe that the low production costs, coupled with relatively high chemical stability would deem these materials promising for suggested applications.

4. Conclusions

In this work, synthesis and characterization of two high-temperature superconductors YBCO and BSCCO were carried out. The possibility of exploiting these materials as probable electrocatalytic alternatives to platinum was explored via oxygen reduction and hydrogen evolution reactions, two crucial industrial processes for development of energy-storage and fuel cell technologies. Both materials proved to be electroactive in nature, and have exhibited remarkable electrocatalytic performances in ORR and HER. Contrary to the high cost and rarity of platinum, these layered superconductors serve as promising replacements for the former owing to their low cost and high availability. At an economic standpoint, these cost-efficient electrocatalysts also promote the development of cleaner and renewable energy applications in future.

Acknowledgements

M.P. acknowledges Tier 2 grant (MOE2013-T2-1-056) from Ministry of Education, Singapore. Z.S. and O.J. were supported by Czech science foundation (GACR No. 13-17538S) and by Specific university research (MSMT No. 20/2015).

Notes and references

[a] School of Physical and Mathematical Science, Division of Chemistry and Biological Chemistry, Nanyang Technological University, 21 Nanyang Link, Singapore. Email: pumera.research@gmail.com

[b] University of Chemistry and Technology Prague, Department of Inorganic Chemistry, Technická 5, 166 28 Prague 6, Czech Republic.

1 L. Qu, Y. Liu, J. B. Baek and L. Dai, *ACS Nano*, 2010, **4**, 1321.

2 J. Suntivich, H. A. Gasteiger, N. Yabuuchi, H. Nakanishi, J. B. Goodenough and Y. Shao-Horn, *Nat. Chem.*, 2011, **3**, 546.

3 X. Xia, C. Zhu, J. Luo, Z. Zeng, C. Guan, C. F. Ng, H. Zhang and H. J. Fan, *Small*, 2014, **10**, 766.

4 C. Xu, B. Xu, Z. Xiong, J. Sun and X. S. Zhao, *Energy Environ. Sci.*, 2013, **6**, 1388.

5 J. D. Benck, T. R. Hellstern, J. Kibsgaard, P. Chakthranont and T. F. Jaramillo, *ACS Catal.*, 2014, **4**, 3957.

6 R. Parsons, *Trans. Faraday Soc.*, 1958, **54**, 1053.

7 G. Wu and P. Zelenay, *Acc. Chem. Res.*, 2013, **46**, 1878.

8 Y. Zheng, Y. Jiao, M. Jaroniec, Y. Jin and S. Z. Qiao, *Small*, 2012, **8**, 3550.

9 Y. L. Zheng, D. Mei, Y.-X. Chen and S. Ye, *Electrochem. Commun.*, 2014, **39**, 19.

10 B. E. Conway and B. V. Tilak, *Electrochim. Acta.*, 2002, **47**, 3571.

11 S. Guo, S. Zhang, D. Su and S. Sun, *J. Am. Chem. Soc.*, 2013, **135**, 13879.

12 H. Zhu, S. Zhang, Y.-X. Huang, L. Wu and S. Sun, *Nano Lett.*, 2013, **13**, 2947.

13 Y. Li, H. Wang, L. Xie, Y. Liang, G. Hong and H. Dai, *J. Am. Chem. Soc.*, 2011, **133**, 7296.

14 M. Jahan, Z. Liu and K. P. Loh, *Adv. Funct. Mater.*, 2013, **23**, 5363.

15 X.-Y. Zhang, H.-P. Li, X.-L. Cui and Y. Lin, *J. Mater. Chem.,* 2010, **20**, 2801.

16 Z.-H. Sheng, H.-L. Gao, W.-J. Bao, F.-B. Wang and X.-H. Xia, *J. Mater. Chem.,* 2012, **22**, 390.

17 D. Voiry, H. Yamaguchi, J. Li, R. Silva, D. C. B. Alves, T. Fujita, M. Chen, T. Asefa, V. B. Shenoy, G. Eda and M. Chhowalla, *Nature Mater.*, 2013, **12**, 850.

18 Z. Sofer, O. Jankovský, P. Šimek, K. Klímová, A. Macková and M. Pumera, *ACS Nano*, 2014, **8**, 7106.

19 A. Martin, J. Hernández-Ferrer, L. Vázquez, M-T. Matínez and A. Escarpa, *RSC Adv*, 2014, **4**, 132.

20 C. S. Lim, C. K. Chua, Z. Sofer, O. Jankovský and M. Pumera, *Chem. Mater.*, 2014, **26**, 4130.

21 O. Jankovský, D. Sedmidubský, K. Rubešová, Z. Sofer, J. Leitner, K. Ružička and P. Svoboda, *Thermochimica. Acta.*, 2014, **582**, 40.

22 B. A. Albiss and I. M. Obaidat, *J. Mater. Chem.* 2010, **20**, 1836.

23 T. Akachi, R. Escudero, R. A. Barrio, D. Ríos-Jara and L. Baños, *J. Phys. C: Solid State Phys.*, 1988, **21**, 2565.

24 H. Maeda, Y. Tanaka, M. Fukutomi and T. Asano, *Jpn. J. Appl. Phys.*, 1988, **27**, 1209.

25 C. Lin, G. Lu, Z.-X. Liu, Y.-X. Sun, J. Lan. G.-Z. Li, S.-Q. Feng, C.-D. Wei, Z.-Z. Gan, Z.-Y. Liu, X.-M. Zheng and B.-X. Lin, *Solid State Commun.*, 1987, **63**, 1129.

26 C. Namgung, J. T. S. Irvine, E. E. Lachowski and A. R. West, *Supercond. Sci. Technol.*, 1989, **2**, 140.

27 B. V. Crist, *Handbooks of Monochromatic XPS Spectra. Volume 2—Commercially Pure Binary Oxides*, XPS International LLC, Leona, Tex, USA, 2005.

28 H. VanDoveren and J. A. T. H. Verhoeven, *J. Electron. Spectrosc. Relat. Phenom.*, 1980, **21**, 265.

29 J. Beyer, Th. Schurig, S. Menkel, Z. Quan and H. Koch, *Physica C*, 1995, **246**, 156.

30 J. J. Yeh, I. Lindau, J. Z. Sun, K. Char, N. Missert, A. Kapitulnik, T. H. Geballe and M. R. Beasley, *Phys. Rev. B* ,1990, **B42**, 8044.

31 P. Srivastava, B. R. Sekahr, N. L. Saini, S. K. Shama, K. B. Garg, B. Mercey, Ph. Lecoer and H. Murray, *Solid State Commun.*, 1993, **88**, 105.

32 T.-H. Shen, D. Greig, J. A. D. Matthew, G. Beamson, G. Balakrishnan, C. T. Lin and W. Y. Liang, *Surf. Rev. Lett.*, 1994, **1**, 545.

33 H. M. Meyer III, D. M. Hill, J. H. Weaver, D. L. Nelson and C. F. Gallo, *Phys. Rev.*, 1988, **B38**, 7144.

34 K. Jacobi, C. Astaldi, B. Frick and P. Geng, *Phys. Rev.*, 1987, **B36**, 3079.

35 S. Kohiki, T. Wada, S. Kawashima, H. Takagi, S. Uchida and S. Tanaka, *Phys. Rev.*, 1988, **B38**, 8868.

36 M. Ni and B. D. Ratner, *Surf. Interface Anal.*, 2008, **40**, 1356.

37 N. Wang, Q. Zhang, Y. Wang, M. Ji and X. Liu, *Z. Phys. B – Condensed Matter.*, 1992, **86**, 325.

38 F. Parmigiani and L. Sangaletti, *J. Electron Spectrosc. Relat. Phenom.*, 1994, **66**, 223.

39 Y. Gorlin and T. F. Jaramillo, *J. Am. Chem. Soc.*, 2010, **132**, 13612.

40 J. Masa, C. Batchelor-McAuley, W. Schuhmann and R. G. Compton, *Nano Research*, 2014, **7**, 71.

41 C. C. Mayorga-Martinez, A. Chamorro-Garcia and A. Merkoci, *Biosens. Bioelectron.*, 2014, doi:10.1016/j.bios.2014.05.066.

42 M. Regier, E. Keskin and J. Halbritter, *IEEE Trans. Appl. Supercond.*, 1999, **9**, 2375.

43 J. P. Zhou, S. M. Savoy, R. K. Lo, J. Zhao, M. Arendt, Y. T. Zhu, A. Manthiram and J. T. McDevitt, *Appl. Phys. Lett.*, 1995, **66**, 2900.

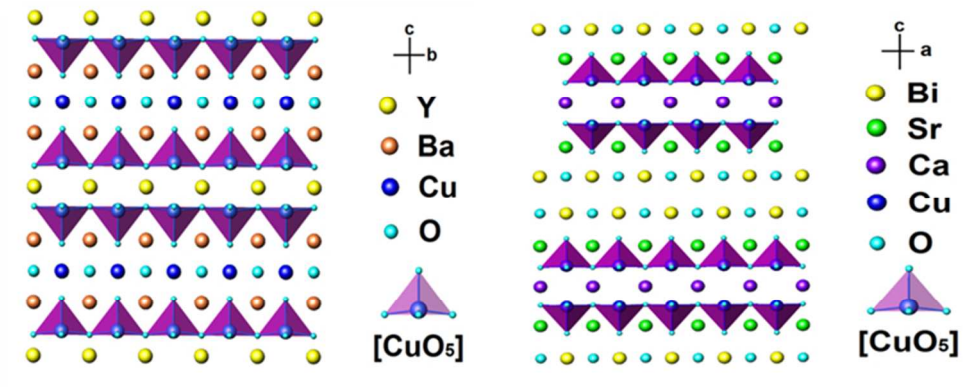
c
b
Y
Ba
Cu
O
[CuO5]
c
a
Bi
Sr
Ca
Cu
O
[CuO5]